ETL-0502

AD-A200 291

DTIC FILE COPY

Improving Classification Accuracy of Radar Image Using a Multiple-*STAGE* Classifier

Neil D. Fox
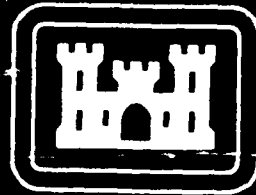Pi-Fuay Chen

September 1988

DTIC
SELECTED
OCT 0 4 1988
E

U.S. ARMY CORPS OF ENGINEERS
ENGINEER TOPOGRAPHIC LABORATORIES
FORT BELVOIR, VIRGINIA 22060-5546

88 10 4 076

REPORT DOCUMENTATION PAGE

Form Approved
OMB No. 0704-0188

1a. REPORT SECURITY CLASSIFICATION UNCLASSIFIED	1b RESTRICTIVE MARKINGS

2a. SECURITY CLASSIFICATION AUTHORITY	3 DISTRIBUTION / AVAILABILITY OF REPORT
2b. DECLASSIFICATION / DOWNGRADING SCHEDULE	Approved for Public Release; Distribution is Unlimited.

4. PERFORMING ORGANIZATION REPORT NUMBER(S)	5. MONITORING ORGANIZATION REPORT NUMBER(S)
ETL-0502	

6a. NAME OF PERFORMING ORGANIZATION U.S. Army Engineer Topographic Laboratories	6b. OFFICE SYMBOL (If applicable) CEETL-RI	7a. NAME OF MONITORING ORGANIZATION

6c. ADDRESS (City, State, and ZIP Code) Fort Belvoir, Virginia 22060-5546	7b. ADDRESS (City, State, and ZIP Code)

8a. NAME OF FUNDING / SPONSORING ORGANIZATION	8b. OFFICE SYMBOL (If applicable)	9. PROCUREMENT INSTRUMENT IDENTIFICATION NUMBER

8c. ADDRESS (City, State, and ZIP Code)	10. SOURCE OF FUNDING NUMBERS			
	PROGRAM ELEMENT NO. 6.11.02A	PROJECT NO. B52C	TASK NO. B	WORK UNIT ACCESSION NO. 015

11. TITLE (Include Security Classification)

Improving Classification Accuracy of Radar Images Using a Multiple-STAGE Classifier

12. PERSONAL AUTHOR(S)
Neil D. Fox and P.F. Chen

13a. TYPE OF REPORT Research Note	13b. TIME COVERED FROM Jun 84 TO Dec 84	14. DATE OF REPORT (Year, Month, Day) 1988, September	15. PAGE COUNT 20

16. SUPPLEMENTARY NOTATION

17. COSATI CODES			18. SUBJECT TERMS (Continue on reverse if necessary and identify by block number)
FIELD	GROUP	SUB-GROUP	Radar Image Feature Extraction, Texture, Histogram, Classification. Pattern Recognition, Edge Operators.

19. ABSTRACT (Continue on reverse if necessary and identify by block number)

A simple method was introduced to classify radar image samples repeatedly for achieving a higher accuracy than by using a single-stage classifier. A Sobel edge operator was applied between the stages of classification to enhance the difference in texture between categories of radar image samples, thus reducing the overlap of image categories.

20. DISTRIBUTION / AVAILABILITY OF ABSTRACT ☒ UNCLASSIFIED/UNLIMITED ☐ SAME AS RPT. ☐ DTIC USERS	21. ABSTRACT SECURITY CLASSIFICATION UNCLASSIFIED
22a. NAME OF RESPONSIBLE INDIVIDUAL E. James Books	22b TELEPHONE (Include Area Code) (202) 355-2774 22c. OFFICE SYMBOL CEETL-IM-T

DD Form 1473, JUN 86   *Previous editions are obsolete.*   SECURITY CLASSIFICATION OF THIS PAGE

UNCLASSIFIED

PREFACE

This work reported on was done under DA Project, 4A161102B52C, Task B, Work Unit 015, "Automated Radar Feature Extraction Research."

The work was performed during the period June 1984 to December 1984 under the supervision of Dr. Frederick W. Rohde, Team Leader, Center for Automated Image Analysis, and Mr. Lawrence A. Gambino, Director, Research Institute.

COL David F. Maune, EN, was Commander and Director, and Mr. Walter E. Boge was Technical Director of the U.S. Army Engineer Topographic Laboratories during the report preparations.

Accession For	
NTIS GRA&I	☒
DTIC TAB	☐
Unannounced	☐
Justification	
By	
Distribution/	
Availability Codes	
Dist	Avail and/or Special
A-1	

CONTENTS

IMPROVING CLASSIFICATION ACCURACY OF RADAR IMAGES USING A MULTIPLE-STAGE CLASSIFIER

INTRODUCTION

In a previous report[1], a Bayes classifier[2] was applied to classify samples of SAR (Synthetic Aperture Radar) imagery obtained from the Huntsville, AL, and the Elizabeth City, NC, areas at the U.S. Army Engineer Topographic Laboratories. The feature vector used for classification was developed based on texture and histogram measurements of each image sample. Each image sample was classified as one of the following four terrain categories: field, water, forest, or city. A highest overall classification accuracy of 95.5 percent was obtained for the 400 samples selected from the Huntsville, AL, imagery set. However, the same method failed to produce a satisfactory accuracy for the other set of imagery. This failure was mainly due to the insufficient measurable differences of image texture appearing between the categories of fields and forests from the Elizabeth City, NC, imagery set. The problem was solved by repeatedly classifying image samples by using a multiple-stage classifier. This report illustrates how a two-stage classifier, together with a Sobel edge operator between the stages, can be used to improve classification accuracy to achieve a highly successful value of 97.75 percent.

METHODOLOGY

The images used for this experiment consisted of 400 samples, each of high resolution SAR imagery taken over the Huntsville, AL, and Elizabeth City, NC, areas with the APD-10 and UPD-4 radar systems, respectively. The digitized image samples were stored on the disk of a Hewlett-Packard 1000 minicomputer system, which includes, besides the disk, a magnetic tape unit, a line printer, a system console, and three other satellite CRT (Cathode-Ray Tube) terminals. A Lexidata System 3400 display processor is also tailored as a peripheral of this system for displaying images of various sizes at different processed stages. Each image sample consisted of 32- by 32-pixels. This window size was used throughout the entire experiment. Each window contained an image sample of one particular terrain category. The four terrain categories considered were (1) cities (combination of commercial and residential structures, DLMS Category #504 FIC 301 and #505 FIC 401), (2) fields (agriculture used primarily for crops and pasture land, DLMS Category #510 FIC 950), (3) water (rivers with smooth fresh water, DLMS Category #510 FIC 940 and fresh water subject to ice, such as lakes and reservoirs, DLMS Category #510 FIC 943), and (4) forests (mixed trees, such as deciduous and evergreens, DLMS Category #510 FIC 954). A feature vector consisting of 15 components was computed for each image sample. The components of the feature vector were established based on the first- and second-order histogram statistics calculated from the 32- by 32-pixel window. The equations for these histogram and texture measurements are provided in appendix A. Taking the feature vector as the input, a Bayes classifier was used to classify each image sample into one of the four terrain categories as described above. The block diagram of the scheme is shown in figure 1.

---

[1] Richard A. Hevenor and Pi-Fuay Chen. Pattern Classification Techniques Applied to Samples of High Resolution Synthetic Aperture Radar Imagery, U.S. Army Engineer Topographic Laboratories, Fort Belvoir, Virginia, ETL-0443, AD A-183537, 1986.

[2] J.T. Tou and R.C. Gonzales, Pattern Recognition Principles, Addison-Wesley Publishing Company, Inc., Reading, Massachusetts, 1974.

With this scheme, the 400 image samples selected from the Huntsville, AL, imagery set were classified correctly with an overall accuracy of 95.5 percent. However, the same scheme failed to yield a successful classification rate for the other set of image samples from Elizabeth City, NC. It was found that the statistics computed from the categories of fields and forests were very similar. In order to overcome this problem, the original scheme was modified as shown in figure 2. An edge operator and a second stage classifier were added. An image sample classified as either a "field" or a "forest" is now channeled through an edge operator, which in this case is a Sobel operator, to yield a pattern of more pronounced texture. Appendix B describes the Sobel operator. The edge-enhanced image sample is then classified a second time with a classifier of any type. For the case illustrated in this report, a simple average routine and a threshold were applied to divide the category of fields from the category of forests since image samples after edge-enhancement were completely separated into two categories.

RESULTS

Two sets of image samples described in the previous section were used as input for the system (scheme) shown in figure 1. Each set consisted of 400 samples that came from four terrain categories. The terrain categories were fields, water, forests, and cities. One hundred image samples were selected randomly from each category. The classification accuracy was evaluated for each category of the terrain feature for various integer-scanning directions (IDIR) and inter-pixel spacings (IPS). The IDIR and IPS were two parameters used to compute the joint-probability matrices during the feature measurement stage, which precedes the classification. See appendix C for more details on IDIR, IPS, and joint-probability matrix. The overall classification accuracy was then calculated for each combination of these two parameters. It was found that for the sample set, from Huntsville, AL, the best overall classification accuracy of 95.50 percent was obtained for the case when the IDIR and IPS were set equal to 0 degree and 2 pixels, respectively, and for another case when the IDIR was 135 degrees and the IPS was 3 pixels. The least accurate case for this set was 92.95 percent, which occurred when the IDIR was 90 degrees and the IPS was 1 pixel. In figures 3 and 4, the classification results are shown for each terrain category for these two extreme cases.

The same scheme, however, failed to produce satisfactory recognition rates for the samples from the Elizabeth City, NC, area. The classification results for the best and worst cases are shown in figures 5 and 6. It was discovered that, for all cases considered, many forest image samples were misclassified as fields because of the smooth appearance of the forest texture from this imagery set (see figures 5 and 6). The highest and lowest overall classification accuracy illustrated in figures 5 and 6 are 87.50 percent and 78.50 percent, respectively.

In order to overcome this problem, the system was modified as shown in figure 2, and the same set of image samples from Elizabeth City, NC, was evaluated again by this modified system. Figure 7 illustrates the classification results obtained for the image samples from Elizabeth City, NC, using the modified new scheme. It is seen that the overall classification accuracy has been improved from 87.50 percent to a highly successful value of 97.75 percent. The same scheme shown in figure 2 was used to rerun the image samples from the Huntsville, AL, area. A nearly perfect overall classification accuracy of 99.25 percent was obtained. Only three samples among a total of 400 samples were misclassified in this case. The results of this classification are shown in figure 8.

2

DISCUSSION

Further research and experimentation is required to verify whether the technique described can be extended to more than two stages of classification to obtain an even higher classification accuracy. It would also be useful to see if the application of a filter, other than an edge operator, may be used advantageously between successive stages.

The possible limitation of the scheme described in this report is the requirement of training whenever a new set of image samples is to be classified with reasonably high accuracy.

CONCLUSIONS

A technique of repeated classification can be used to improve the classification accuracy for selected sets of terrain features on SAR imagery. This classification method is very effective because it produces a significantly higher classification accuracy than the Bayes classifier with only 5 to 10 percent additional computer time.
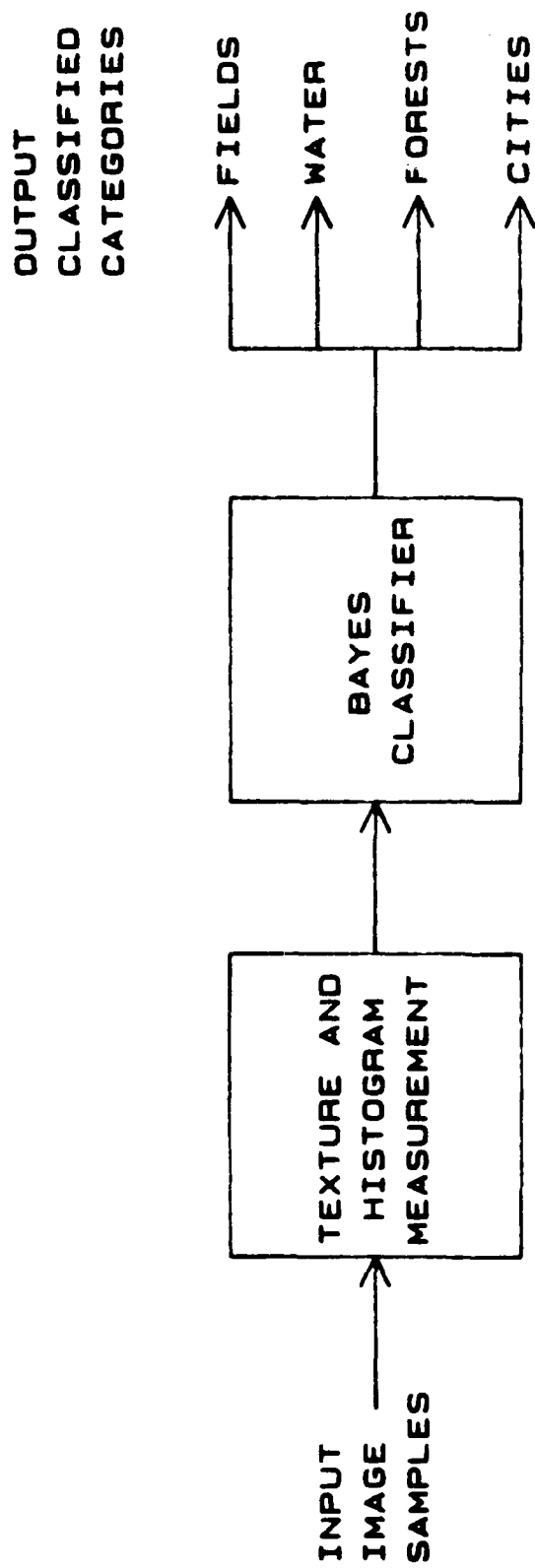
Figure 1. Original System Diagram.

4

FIRST STAGE
CLASSIFIED
CATEGORIES

INPUT IMAGE
SAMPLES →

TEXTURE AND HISTOGRAM MEASUREMENT	→	FIRST STAGE CLASSIFIER (BAYES)

→ WATER

FORESTS

AND

FIELDS

→ CITIES

SOBEL EDGE OPERATOR	→	SECOND STAGE CLASSIFIER (AVERAGE AND THRESHOLD)

→ FIELDS

→ FOREST!

Figure 2. Modified System Diagram.

5

TRUE CAT / REC CAT	FIELD	WATER	FOREST	CITY
FIELD	88	0	2	1
WATER	0	100	0	0
FOREST	9	0	98	1
CITY	3	0	2	88

OVERALL CLASSIFICATION ACCURACY = 95.50%

IPS= 2 PIXELS   IDIR= 0 DEGREES

Figure 3. The Best Overall Classification Accuracy for Image Samples from Huntsville, AL, with a Single-Stage Classifier.

TRUE CAT / REC CAT	FIELD	WATER	FOREST	CITY
FIELD	89	0	6	7
WATER	0	100	0	0
FOREST	9	0	81	2
CITY	2	0	3	81

OVERALL CLASSIFICATION ACCURACY = 92.75%

IPS= 1 PIXEL   IDIR= 90 DEGREES

Figure 4. The Worst Overall Classification Accuracy for Image Samples from Huntsville, AL, with a Single-Stage Classifier.

7

TRUE CAT / REC CAT	FIELD	WATER	FOREST	CITY
FIELD	97	0	35	8
WATER	0	100	0	0
FOREST	3	0	62	1
CITY	0	0	3	91

OVERALL CLASSIFICATION ACCURACY = 87.50 %

IPS= 1 PIXEL   IDIR= 90 DEGREES

Figure 5. The Best Overall Classification Accuracy for Image Samples from Elizabeth, NC, with a Single-Stage Classifier.

8

TRUE CAT / REC CAT	FIELD	WATER	FOREST	CITY
FIELD	98	0	88	11
WATER	0	100	0	0
FOREST	1	0	28	1
CITY	1	0	4	88

OVERALL CLASSIFICATION ACCURACY = 78.50%

IPS= 4 PIXELS   IDIR= 45 DEGREES

Figure 6.   The Worst Overall Classification Accuracy for Image Samples from Elizabeth City, NC, with a Single-Stage Classifier.

9

TRUE CAT \ REC CAT	FIELD	WATER	FOREST	CITY
FIELD	89	0	0	0
WATER	0	100	0	0
FOREST	1	0	84	3
CITY	0	0	8	97

OVERALL CLASSIFICATION ACCURACY = 97.75%

IPS= 3 PIXELS   IDIR= 90 DEGREES

Figure 7. The Best Overall Classification Accuracy for Image Samples from Elizabeth City, NC, with a Multiple-Stage Classifier.

TRUE CAT / REC CAT	FIELD	WATER	FOREST	CITY
FIELD	98	0	0	0
WATER	0	100	0	0
FOREST	1	0	98	0
CITY	0	0	2	100

OVERALL CLASSIFICATION ACCURACY = 99.25 %

IPS= 1 PIXEL   IDIR= 0 DEGREE

Figure 8.   The Best Overall Classification Accuracy for Image Samples from Huntsville, AL., with a Multiple-Stage Classifier.

11

APPENDIX A. FEATURE VECTOR COMPONENTS

Many publications are available on the image-statistics-processing techniques. The most concise form of the feature vector based on the first- and second- order image pixel amplitude distribution was given by Pratt.[3] He defined a discrete image array, F(j,k), and the first-order probability distribution of image amplitude of a measurement window centered about (j,K) as

$$P(b) = \frac{N(b)}{M}$$

where M represents the total number of pixels in the measurement window, N(b) is the number of pixels of amplitude b in the window, and $0 < b < L - 1$, and L is the number of gray levels of F(j,k). The following measures have been formulated by Pratt as a concise means of describing the shape of first-order image histograms:

$$\text{Mean} \quad \bar{b} = \sum_{b=0}^{L-1} b \, P(b)$$

$$\text{Variance} \quad \sigma_b^2 = \sum_{b=0}^{L-1} (b - \bar{b})^2 \, P(b)$$

$$\text{Skewness} \quad b_s = \frac{1}{\sigma_b^3} \sum_{b=0}^{L-1} (b - \bar{b})^3 \, P(b)$$

$$\text{Kurtosis} \quad b_k = \frac{1}{\sigma_b^4} \sum_{b=0}^{L-1} (b - \bar{b})^4 \, P(b) - 3$$

$$\text{Energy} \quad b_N = \sum_{b=0}^{L-1} [\, P(b) \,]^2$$

$$\text{Entropy} \quad b_E = - \sum_{b=0}^{L-1} P(b) \, \log_2 [\, P(b) \,]$$

---

[3]W.K. Pratt, _Digital Image Processing_, John Wiley and Sons, Inc., New York, 1978.

The second-order histogram features are based on the definition of the joint probability distribution of pairs of pixels. Pratt stated that the two-dimensional histogram can be considered as an estimate of joint probability distribution. Consider a pair of pixels $F(j,k)$ and $F(m,n)$ that are separated by γ radial units, at an angle θ with respect to the x-axis of the measurement window. The histogram estimate of the second order distribution is given by Pratt as

$$P(a,b) = \frac{N(a,b)}{M}$$

where M is the total number of all occurrences in the measurement window, and where $N(a,b)$ is the number of occurrences for which $F(j,k)=a$, $F(m,n)=b$. The following are the texture measures that were used in this study:

$$\text{Mean:} \qquad \bar{a} = \sum_{a=0}^{L-1} \sum_{b=0}^{L-1} a\, P(a,b)$$

$$\bar{b} = \sum_{a=0}^{L-1} \sum_{b=0}^{L-1} b\, P(a,b)$$

$$\text{Variance:} \qquad V_a = \sum_{a=0}^{L-1} \sum_{b=0}^{L-1} (a-\bar{a})^2\, P(a,b)$$

$$V_b = \sum_{a=0}^{L-1} \sum_{b=0}^{L-1} (b-\bar{b})^2\, P(a,b)$$

$$\text{Covariance:} \qquad C_o = \sum_{a=0}^{L-1} \sum_{a=0}^{L-1} (a-\bar{a})(b-\bar{b})\, P(a,b)$$

14

Autocorrelation: $$A_u = \sum_{a=0}^{L-1} \sum_{b=0}^{L-1} a\, b\, P(a, b)$$

Absolute Value: $$A_b = \sum_{a=0}^{L-1} \sum_{b=0}^{L-1} |a - b|\, P(a, b)$$

Energy: $$E_g = \sum_{a=0}^{L-1} \sum_{b=0}^{L-1} [P(a, b)]^2$$

Inverse Difference: $$I_d = \sum_{a=0}^{L-1} \sum_{b=0}^{L-1} \frac{P(a, b)}{1 + (a - b)^2}$$

Inertia: $$I_n = \sum_{a=0}^{L-1} \sum_{b=0}^{L-1} (a - b)^2\, P(a, b)$$

Entropy: $$E_n = -\sum_{a=0}^{L-1} \sum_{a=0}^{L-1} p(a, b)\, \log_2 [P(a, b)]$$

For our application the joint-probability matrix was made to be symmetrical so that $a = b$, and $V_a = V_b$.

APPENDIX B. SOBEL EDGE OPERATOR

The Sobel operator is a 3- by 3-pixel nonlinear edge enhancement mask which is multiplied sequentially with all pixel values in a given image to produce a pattern of pronounced edges.

The weights for the Sobel mask are shown below:

-1	0	1		1	2	1
-2	0	2		0	0	0
-1	0	1		-1	-2	-1

| x-direction | y-direction |

Assume a block of 3- by 3-pixels to be multiplied with the Sobel mask centered at the point (i.j) and having a gray-value distribution as given below:

$$A_0 \quad A_1 \quad A_2$$

$$A_7 \quad F(i.j) \quad A_3$$

$$A_6 \quad A_5 \quad A_4$$

Then, the magnitude of the resultant pixel, G(i,j), which is to replace F(i,j) will be

$$|G (i,j)| = \sqrt{X^2 + Y^2},$$

where $\quad X = (A_2 + 2A_3 + A_4) - (A_0 + 2A_7 + A_6),$

and $\quad Y = (A_0 + 2A_1 + A_2) - (A_6 + 2A_5 + A_4).$
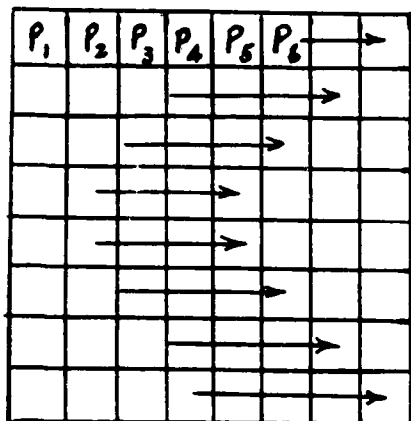
17

APPENDIX C. JOINT-PROBABILITY MATRIX AND ITS PARAMETERS, IDIR AND IPS

A joint-probability matrix, which represents the joint probability of gray-level occurrence for a pair of pixels in a given image, is a way to facilitate texture measurement of an image. To compute a joint-probability matrix for a given image, or a window of pixels, it is required to consider at least two basic parameters. These are the integer-scanning directions (IDIR), and the integer-pixel spacings (IPS).
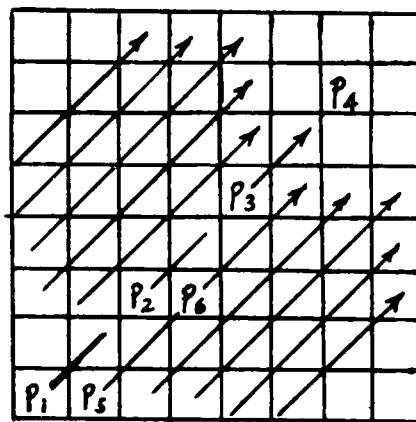
The IDIR are the directions along which a pair of pixels are sequentially selected for computing the joint-probability of gray-level-occurrence, and the IPS are the integer spacings between pair of pixels. Thus, an IDIR can be represented by an angle between a scan line and the bottom edge of the pixel window. Since a pixel-window size of 32 by 32 was used, theoretically the IPS can assume numbers 1 through 31. However, for practicality we have only computed the joint-probability matrices for the cases where the IPS values were 1 through 6, and IDIR were set equal to 0, 45, 90, and 135 degrees.

The following figures illustrate the cases with various IDIR and IPS values. For simplicity, the pixel windows are shown to be 8 by 8. The arrows show scan lines, while pixels are identified by p's. Steps for computing a joint-probability matrix are listed below:
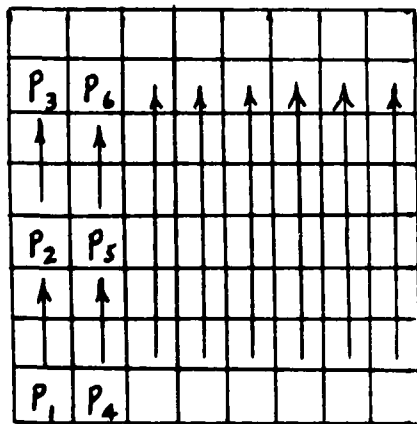
1. Select pixels p_1 and p_2, and record their joint-occurrence of gray levels (e.g. if the gray level of p_1 and p_2 are assumed to be 7 and 10 respectively, then the joint-occurrence of gray levels 7 to 10 is recorded once).

2. Follow the arrow to record the joint-occurrence of gray levels for the pairs of pixels, p_2 and p_3, p_3 and p_4, and so on until the edge pixel of the pixel window is examined.

3. Repeat steps 1 and 2 for the rest of the scan lines until all available pixels in the pixel-window have been taken into consideration.

4. Add up numbers of joint-occurrences for each permuted gray level obtained in the steps 1 to 3, and then compute the joint-probability matrix for the entire pixel window. Each element of this matrix will be a decimal number obtained by dividing the total number of joint-occurrences for a particular permuted gray level by the total number of all joint-occurrences.
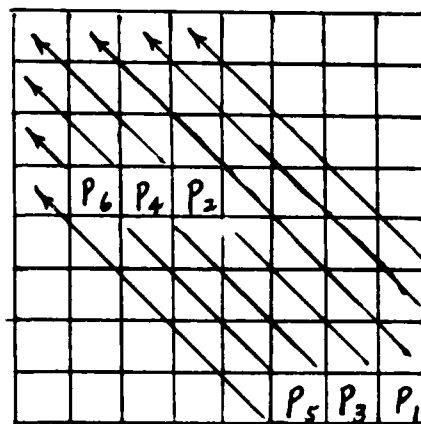
19

IDIR = 0 degree, IPS = 1 pixel.

IDIR = 45 degrees, IPS = 2 pixels.

IDIR = 90 degrees, IPS = 3 pixels.

IDIR = 135 degrees, IPS = 4 pixels.